GEOLOGIC STORAGE OF CARBON DIOXIDE: AN EXPERIMENTAL STUDY OF PERMANENT CAPILLARY TRAPPING AND RELATIVE PERMEABILITY

M. Akbarabadi and M. Piri
Department of Chemical & Petroleum Engineering, University of Wyoming, Dept. 3295, 1000 E. University Ave., Laramie, WY 82071-2000, USA

This paper was prepared for presentation at the International Symposium of the Society of Core Analysts held in Austin, Texas, USA 18-21 September, 2011

ABSTRACT

We present the results of an extensive experimental study on the effects of hysteresis on permanent capillary trapping and relative permeability of CO_2/brine systems. We performed numerous unsteady- and steady-state drainage and imbibition full-recirculation flow experiments in three different sandstone rock samples, i.e., low- and high-permeability Berea, and Nugget. A state-of-the-art reservoir conditions core-flooding system was used to perform the tests. This system included nine cylinders Quizix pumping system that allowed full-recirculation experiments with tightly controlled flow and pressure conditions leading to a superior equilibrium between CO_2 and brine. The core-flooding apparatus also included a medical CT scanner to measure in-situ saturations. The scanner was rotated to the horizontal orientation allowing flow tests through vertically-placed core samples with about 3.8 cm diameter and 15 cm length. Both supercritical-CO_2/brine and gaseous-CO_2/brine fluid systems ($scCO_2$ & gCO_2) were studied. The gaseous and supercritical CO_2/brine experiments were carried out at 502 and 1595.5 psig back pressures and 20 and 55 °C temperatures, respectively. Under the above-mentioned conditions, the gCO_2 and $scCO_2$ have 0.081 and 0.393 gr/cm^3 densities, respectively. The samples were first saturated with brine and then flooded with CO_2 (drainage) at different maximum flow rates. The drainage process was then followed by a low flow rate (0.375 cm^3/min) imbibition until residual CO_2 saturation was achieved. Wide flow rate ranges of 0.25 to 20 cm^3/min for $scCO_2$ and 0.125 to 120 cm^3/min for gCO_2 were used to investigate the variation of irreducible brine saturation (S_{wirr}) with maximum CO_2 flow rate and variation of trapped CO_2 saturation (S_{CO2r}) with Swirr. For a given S_{wirr}, the trapped $scCO_2$ saturation was less than that of gCO_2 in the same sample. This was attributed to brine being less wetting in the presence of $scCO_2$ than in the presence of gCO_2. The ratio of S_{CO2r} to initial CO_2 saturation (1- S_{wirr}) was found to be much higher for low initial CO_2 saturations. This means that greater fractions of injected CO_2 can be permanently trapped at higher initial brine saturations. The results indicate that very promising fractions (about 50 to 70 %) of the initial CO_2 saturation can be permanently trapped. Maximum CO_2 and brine relative permeabilities at the end of

drainage and imbibition and also variation of brine relative permeability due to post-imbibition CO_2 dissolution were also studied.

INTRODUCTION

Capturing CO_2 from stationary sources and injecting it into underground geologic formations for storage purposes is currently receiving significant attention as a potentially viable option for geologic storage and ultimate sequestration of significant quantities of CO_2. Among various geologic formations, deep saline aquifers are considered important CO_2 sinks because of their potential storage capacity for large volumes of carbon dioxide. The International Energy Agency (IEA) has reported that saline aquifers have a global storage capacity of 400-10,000 Gt of CO_2 [1].

In the sequestration process, CO_2 captured from commercial or industrial operations is injected into deep salt water aquifers, where it may exist as supercritical fluid, to prevent atmospheric residence of CO_2. Carbon dioxide injected into a geologic formation may be sequestrated through three mechanisms: (1) CO_2 may stay in its own phase but in two topological forms, A) as a large continuous plume which moves while more CO_2 is injected. At the pore-level, this is equivalent to well-connected CO_2 clusters that reside at the center of the pores and throats. B) Sftagnant residual CO_2. This is the CO_2 that gets trapped due to, for instance, invasion of brine after CO_2 injection is terminated. It is a consequence of displacement process named imbibition that may take place due to pressure gradients, background velocity of aquifer or water injection. During this process, CO_2 gets trapped due to pore-level displacement mechanisms such as snap-off or by-passing of CO_2. (2) CO_2 can also dissolve in brine forming an acidic solution. The amount of dissolution is controlled by pressure, temperature, salinity of brine, dispersion, and Darcy velocity of the aqueous phase. (3) Acidic solution formed owing to dissolution of CO_2 in brine may react with the hosting rocks producing secondary minerals that may precipitate indirectly sequestrating carbon. These reactions are relatively slow and therefore this sequestration mechanism becomes important over larger time scales. Carbon sequestrated through this mechanism, however, has the lowest risk of leakage.

From the above-mentioned sequestration mechanisms, it is evident that capillary trapping of CO_2 is a very important short-term storage mechanism with a low risk of leakage. In recent years, researchers have intensified the investigations of CO_2/brine displacements and their flow properties. Bennion and Bachu [2-5] studied relative permeabilities of drainage and imbibition processes for $scCO_2$/brine systems under various pressure, temperature, IFT, and fluid compositions in different rock samples using unsteady-state method. Okabe *et al.* [6] performed one complete unsteady-state drainage and imbibition experiment with $scCO_2$/brine core-flooding to study distribution of supercritical $scCO_2$ saturation along the core sample utilizing a medical CT-scanner to measure in-situ saturations. The rock sample was from a carbonate reservoir in the Middle East. Suekane *et al.* [7] performed seven unsteady-state experiments to measure trapped $scCO_2$ saturation in a Berea sandstone core. Perrin *et al.* [8,9] conducted four steady-state drainage experiments with $scCO_2$/brine in two rock samples, Berea sandstone and a sample from south-west of Australia. Shi *et al.* [10] performed one unsteady-state

drainage $scCO_2$/brine core-flooding experiment in a Tako sandstone core. All the above-mentioned studies were performed at relatively low CO_2 flow rates leading to high "irreducible" brine saturations at the end of drainage process. And this has been a limiting factor in the study of capillary trapping due to post-drainage brine injection. One would need to establish a wide range of initial brine saturations prior to the imbibition process to study its impact on trapping. This is the main focus of the experimental study presented in this document. In this work, we investigate the amount of supercritical CO_2 that can be trapped under wide range of flow conditions used during drainage. This paper is structured as follows. First, we provide details of core sample, fluids, and experimental conditions. This is then followed by sections on experimental apparatus and procedure used in this study. The section on results and discussion is presented next. We include two large groups of results for displacement of brine due to CO_2 injection and trapping of CO_2 due to chase brine floods. We study two sandstone samples, Berea and Nugget. We present results for both supercritical and gaseous CO_2 and discuss the differences observed using pore-level displacement mechanisms. Finally, a section on dissolution of trapped supercritical CO_2 is included that shows the distribution of fluids along the length of the samples at various stages of dissolution process.

ROCK SAMPLES, FLUIDS, AND EXPERIMENTAL CONDITIONS

The flow experiments included series of unsteady-state CO_2 (drainage) and brine flooding (imbibition) tests in two different core samples, Berea and Nugget sandstones. Table 1 lists dimensions and other basic petrophysical properties of the cores. Both samples were outcrop cores and strongly water-wet. Nugget sandstone core was obtained from SW Wyoming, while the Berea core was cut from a block obtained from a quarry in Ohio. In this work, we used CO_2 and brine with 10 wt% NaI, 5 wt% NaCl, and 0.5 wt% $CaCl_2$ composition. The experiments with gaseous CO_2 (gCO_2) and brine were carried out at ambient temperature and 502 psig back pressure. Each drainage experiment was started from brine saturated core (S_w=1) with a pre-specified maximum CO_2 flow rate to reach an "irreducible" brine saturation. This was then followed by injection of brine to trap CO_2. We used a wide range of maximum CO_2 flow rates to establish a wide range of initial brine saturation prior to imbibition tests. All the flow rates used in this study are listed in Table 2 for both samples. We performed a total of 46 drainage and imbibition flow tests. At the end of each imbibition experiment, the trapped CO_2 was dissolved by injection of a slightly undersaturated brine to establish S_w=1 for the next drainage test. The same steps were used for experiments with $scCO_2$ and brine. In this group, we used 55 °C temperature and 1595.5 psig back pressure leading to a supercritical condition for CO_2.

EXPERIMENTAL SETUP

The experimental setup used in this work is a state-of-the-art reservoir conditions multiphase core-flooding system that includes nine cylinder Quizix pumping system (5000 and 6000 series), three in-line viscometers (Cambridge Viscosity), a compensation accumulator, an acoustic three-phase separator, air operated Vindum valves, Rosemount differential pressure transducers, a Hassler type core holder, and Yamato and Blue-M

mechanical convection ovens, see Figure 1 for a schematic flow diagram. All the wetted parts of the apparatus are made of Hastelloy and other corrosion resistant materials. The experimental setup is a closed-loop system that allows fluids to be injected into the core with a wide range of flow rates and at elevated temperatures and pressures.

We used dual-cylinder 5000 and 6000 Quizix pumps for injection of brine and CO_2, respectively. A highly controllable and accurate back pressure regulation system was designed and installed to allow very stable back pressures, even at very high flow rate full-recirculation experiments. The effluent of the core was sent to a large 3500 cm^3 acoustic three-phase separator by the back pressure regulation system. The separator is made of Hastelloy and the level of fluids in it are monitored using acoustic transducers. As we mentioned earlier, the system is a closed loop and we performed all the flow tests under full-recirculation mode. Therefore, it is critical to monitor fluid levels in separator to avoid retraction of wrong fluids to the injection pumps. The pressure of the separator is controlled by a state-of-the-art pressure maintenance system which allowed us to achieve very stable separator pressures leading to stable equilibrium between the phases. We installed special ultra high molecular weight seals in Quizix cylinders to prevent any leakage when working with $scCO_2$. The Overburden pressure was maintained using a single cylinder 5000 Quizix pump. Utilization of a Quizix pump allowed automatic adjustment of overburden pressure with variations in the pore pressure. Rosemount differential pressure transducers were used to measure pressure drop across the cores. A sophisticated control system was utilized to operate the pumps and log the data throughout the experiments. The setup also included a medical CT scanner tuned for petrophysical applications. The scanner was rotated to the horizontal orientation allowing us to carry out the experiments through vertically-placed rock samples. A highly accurate vertical positioning system (VPS) was used to move the core holder vertically from bottom into the gantry.

EXPERIMENTAL PROCEDURE

Before the experiments were carried out, the core flooding systems was pressure calibrated and tested for possible leakage. The basic petrophysical properties of core samples were measured using various techniques, see Table 1. For each set of experiments, a core was placed in a Hassler type core holder with a sleeve. The core was wrapped with several layers of Aluminium foil and Teflon tape to prevent CO_2 diffusion into the sleeve. The core holder was then wrapped with appropriate insulation material and located on the VPS system and moved into the CT scanner. The core holder assembly was flushed with gaseous CO_2 from a pressurized cylinder and then vacuumed. At this stage, the entire core was scanned with 1 mm slice thickness generating about 140-150 slices depending on the length of the core.

The core flooding system was first saturated with brine and CO_2. The system was then pressurized (with additional CO_2) and heated to reach 1,600 psig and 55 °C. At this point, brine and CO_2 pumps were used to re-circulate the fluids by-passing the core holder for 12-24 hours to achieve equilibrium between the phases. The fluids were in continuous

contact in the separator, accumulator, flow lines, and back pressure pump during this step. The core was then saturated with equilibrated supercritical CO_2. The core-holder was heated at its two ends using two highly efficient heat bands and manual controllers. The level of heat was adjusted to obtain the desired temperature at the outlet of the core. The fluid temperature at the inlet was also monitored and controlled using heating tapes utilized on all the tubings outside the ovens. Temperature was monitored in other locations of the systems as well, e.g., inside the separator, inside both ovens, and inside the large compensation accumulator. Flow of supercritical CO_2 through the core was continued for a few hours before it was scanned to acquire CO_2 saturated reference image of the core. After acquisition of CO_2-saturated image of the core, brine was injected into the core, to dissolve the CO_2. This was continued until subsequent scans did not show any "free" CO_2 in the core. Then the entire core was scanned to obtain a brine saturated image of the sample. At this point, the core was ready for the first drainage (CO_2 injection) experiment. CO_2 was then injected into the brine saturated core. The effluent fluids were ultimately sent to the separator and recirculated. For each drainage experiment, we used a maximum flow rate, see Table 2. The flow rate was gradually increased to reach the maximum and maintained at that point until the variations in pressure drop and saturation distribution along the length of the core were insignificant. The brine saturation at this point was reported as "irreducible" saturation for the maximum CO_2 flow rate used. The core at the end of drainage was then subjected to brine injection (imbibition). The maximum brine flow rate for all imbibition experiments was 0.375 cm^3/min. The flow rate was increased gradually to reach this maximum and kept under this condition until all the CO_2 was either displaced or trapped. The core was then scanned to report the residual CO_2 saturation. At this point, the sample was resaturated with extensive injection of slightly undersaturated brine to dissolve the trapped CO_2 and reestablish S_W=1. This process was then followed by a new drainage and imbibition experiments. All the experiments were carried out while the core holder was placed vertically in the CT scanner. The core-flooding system was a closed loop apparatus and operated under full-recirculation condition.

RESULTS AND DISCUSSION

Figure 2 shows variation of maximum CO_2 saturation reached versus CO_2 injection flow rate in both samples. Each data point represent the steady-state achieved at a given CO_2 flow rate in an independent experiment and is averaged in the central 70% of the core. The subfigures show the results for gCO_2/brine and $scCO_2$/brine tests in Berea core and $scCO_2$/brine tests in Nugget core. In all these test groups, maximum CO_2 saturation increases sharply in lower flow rates and then gradually stabilizes. This is expected as it becomes more difficult to displace brine from smaller pores and crevices as brine saturation decreases. Performing the flow experiments with wide ranges of maximum CO_2 flow rate led to wide ranges of initial brine saturation for the subsequent brine injection experiments. For example, maximum $scCO_2$ saturation ranged between 0.32 and 0.60 for flow rates between 0.25 and 20 cc/min in Berea. While maximum gCO_2 saturation ranged between 0.33 and 0.65 for flow rates between 0.125 and 120 cc/min in the same core sample. We performed experiments with gaseous CO_2 to allow us to study

possible effects of wetting on trapping of CO_2 as we will discuss later in this section. As it is seen in Figure 2, for a given flow rate, displacement of brine in Nugget sandstone was more effective than in Berea core. We believe capillary elements in the Nugget core were larger with lower drainage threshold capillary pressures and therefore they were invaded by $scCO_2$ more easily. We were able to obtain an average of 67% $scCO_2$ saturation at 10 cc/min $scCO_2$ flow rate in Nugget compared to about 52% in Berea core for the same flow rate. Table 2 lists all the flow rates used in the experiments performed in Berea and Nugget sandstone cores.

After reaching steady-state at the end of each CO_2 injection experiment, chase brine was injected at about 0.375 cc/min. The brine was saturated with CO_2 under the conditions of the experiments before injection. The injection was continued until residual CO_2 saturation was reached. Multiple scans of the core during this process allowed us to determine this point. We then recorded the in-situ saturation and pressure drop across the core. This process was done after every CO_2 injection experiment discussed earlier in this section creating a wide range of residual CO_2 saturations. Figures 3a and 3b show variations of trapped CO_2 saturation with initial brine saturation for both supercritical and gaseous conditions in the Berea core. It is shown that for a given initial brine saturation, trapped gCO_2 saturation is greater than trapped $scCO_2$ saturation in this sample. Our hypothesis is that brine is less wetting in the presence of $scCO_2$ than in the presence of gCO_2 in the same sample leading to more trapping in gCO_2/brine system. Figure 3c depicts the results for Nugget sandstone core. The residual $scCO_2$ saturation in Nugget is higher than those in Berea for a given initial saturation. We think this may have been caused by higher pore/throat aspect ratio in Nugget that directly affects the amount of trapping through various pore-level displacement mechanisms such as snap-off and pore-body filling. Figure 4 includes some CT slices that show the variation of in-situ $scCO_2$ saturation in different locations along the length of Berea sandstone core. As expected, CO_2 and brine are distributed uniformly in core as it is a homogenous sample. The above-mentioned data indicates that residual $scCO_2$ saturation varies between 20% and 32%, which is about 50% to 70% of the initial CO_2 saturation. Figure 5 shows the variation of this ratio with initial CO_2 saturation for both samples. It is shown that significant fractions of the CO_2 initially in place are trapped.

At the end of each CO_2 (or brine) injection experiment, the steady-state saturations and pressure drop data along the length of the core were recorded when their variations in two consecutive measurements were insignificant. The pressure drop data were then used to calculate endpoint CO_2 (or brine) relative permeabilities. Figure 6 presents variation of endpoint relative permeabilities versus brine/CO_2 saturation for both samples. Supercritical CO_2 exhibits particularly low relative permeability. This is consistent with the drainage relative permeability data presented by Perrin and Benson [9].

For each of the samples, we used one of the residual saturation points for additional tests. We studied the dissolution of trapped $scCO_2$ in brine. We injected slightly under-

saturated brine into the sample at residual saturation until all the $scCO_2$ was dissolved. This was a lengthy process. On average it took 24-48 hrs using different brine flow rates. Brine and $scCO_2$ saturations as well as pressure drop data were recorded during this process until the core was fully saturated with brine. Figure 7 exhibits relative permeability of brine during dissolution of trapped $scCO_2$ in both samples. At the beginning of this process, trapped $scCO_2$ creates significant blockage for the flow of brine leading to small brine relative permeabilities. With injection of under-saturated brine, randomly distributed trapped clusters of $scCO_2$ start shrinking gradually reducing the blockage and improving the flow of brine. This manifests itself in lower brine pressure drops and higher brine relative permeabilities. It is important to mention that we carefully monitored variation of $scCO_2$ saturation along the cores during this process and did not observe noticeable mobilization of trapped $scCO_2$ even at advanced stages of dissolution process. Figure 8 shows variation of $scCO_2$ saturation along the length of the Berea and Nugget sandstone cores with time during dissolution.

CONCLUSIONS

We used a robust and high quality full-recirculation core-flooding system to perform numerous drainage and imbibition CO_2/brine flow experiments in two sandstone core samples. Wide ranges of initial brine saturation were established to allow study of their impact on trapping efficiency of chase brine injection. The results indicated that significant quantities of injected CO_2 can be trapped permanently. Trapping efficiency was between 49 to 78% of CO_2 in place. Trapping efficiency was higher at lower initial CO_2 saturations.

ACKNOWLEDGMENTS

We gratefully acknowledge financial support of DOE, EnCana, Saudi Aramco, the School of Energy Resources and the Enhanced Oil Recovery Institute at the University of Wyoming.

REFERENCES

1- IEA Greenhouse Gas R & D Program, http://www.ieagreen.org.uk/ccs.html

2- Bennion, B., S. Bachu, "Relative permeability characteristics for supercritical CO_2 displacing water in a variety of potential sequestration zones in western Canada sedimentary basin," SPE *95547*, (2005).

3- Bennion, B., S. Bachu, "The impact of interfacial tension and pore size distribution/capillary pressure character on CO_2 relative permeability at reservoir condition in CO_2-Brine systems," SPE *99325*, (2006).

4- Bennion, B., S. Bachu, "Supercritical CO_2 and H_2S-Brine drainage and imbibition relative permeability relationships for inter-granular sandstones and carbonate formations," *SPE 99326*, (2006).

5- Bennion, B., S. Bachu, "Dependence on Temperature, pressure and salinity of the IFT and relative permeability displacement characteristics of CO_2 injected in deep saline aquifers," SPE *102138*, (2006).

6- Okabe, H., Y. Tsuchiya, "Experimental Investigation of Residual CO_2 Saturation Distribution in Carbonate Rocks," *International Symposium of the society of the core analysts in Abu Dhabi*, (2008).

7- Suekane, T., T. Nobuso, S. Hirai, M. Kiyota, "Geological storage of carbon dioxide by residual gas and solubility trapping," *International journal of greenhouse gas control*, (2008) **2**, 58-64.

8- Perrin, J.C., M. Krause, C.W. Kuo, l. Milijkovic, E. Charoba, S. Benson, "Core-scale experimental study of relative permeability properties of CO_2 and brine in reservoir rocks," *Energy Procedia*, (2009) **1**, 3515-3522.

9- Perrin, J.C., S. Benson, "An Experimental Study on the Influence of Sub-Core Scale Heterogeneities on CO_2 Distribution in Reservoir rocks," *Transport in Porous Media*, (2010) **82**, 93-109.

10- Shi, J.Q., Z. Xue, S. Durucan , "History matching of CO_2 core flooding CT scan saturation profiles with porosity dependent capillary pressure," *Advances in Water Resources*, (2009) **1**, 3205-3211.

Table 1: Dimensions and petrophysical properties of the cores used in this study.

Sample	Diameter cm	Length cm	φ (X-ray) %	K_{abs} (Brine) mD	Pore Volume cm^3
Berea sandstone	3.81	15.0	20.08	50	34.34
Nugget sandstone	3.81	14.8	14.28	312	24.09

Table 2: Maximum CO_2 flow rates used in drainage (non-wetting phase injection) experiments. The NWP stands for non-wetting phase and WP stands for wetting phase. The flow rates are in cm^3/min.

Sample	NWP	WP	0.125	0.25	0.5	1	2.5	5	10	15	20	30	60	110	120
Berea SS	$scCO_2$	Brine		●	●	●	●	●	●	●	●				
Berea SS	gCO_2	Brine	●	●	●		●		●			●	●	●	●
Nugget SS	$scCO_2$	Brine		●	●	●	●	●	●						

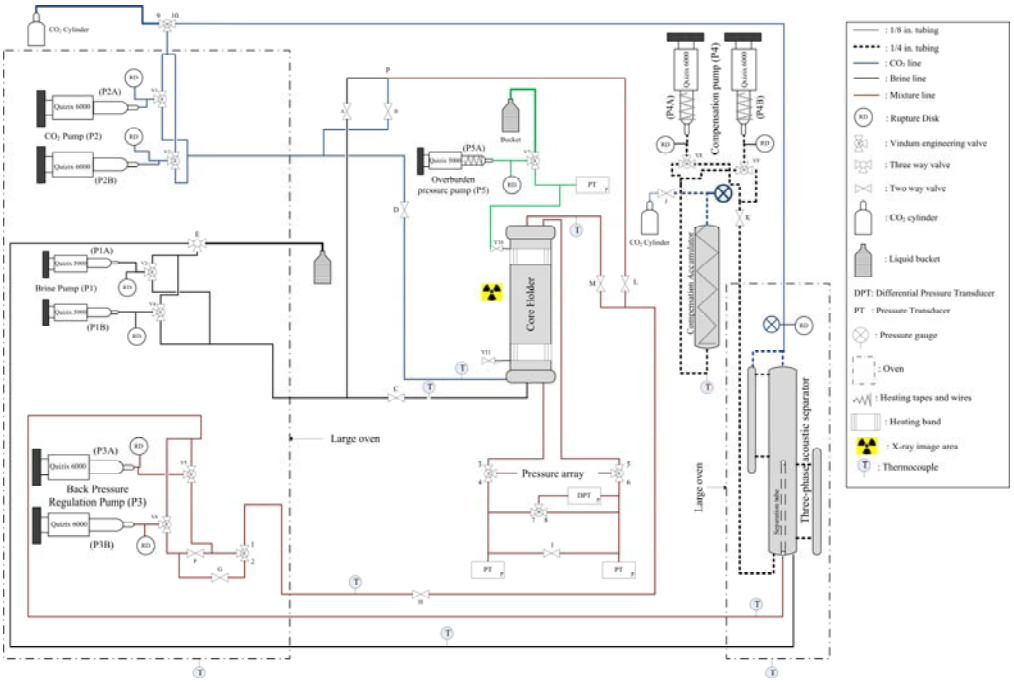

Figure 1 . Schematic flow diagram of the experimental setup used in this work.

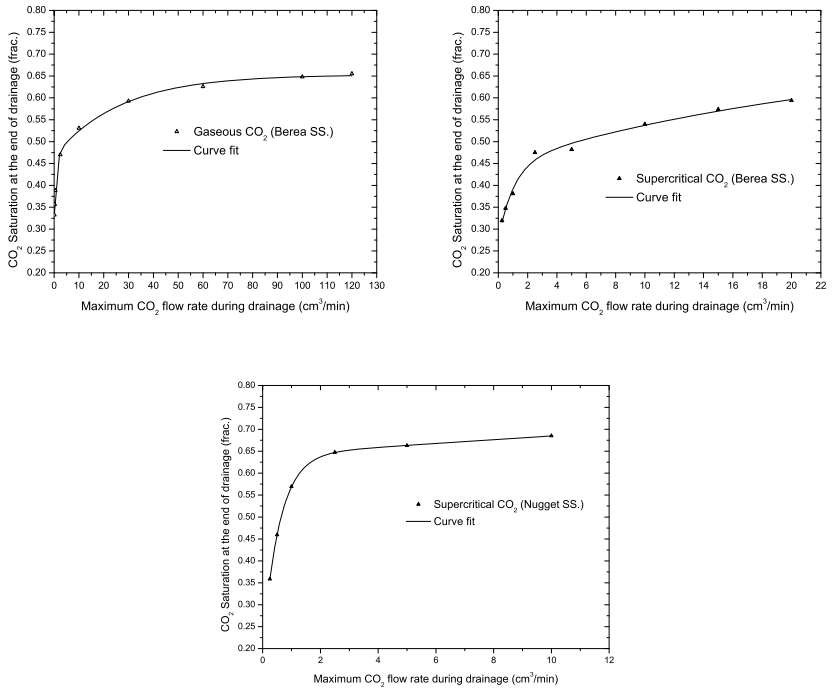

Figure 2. Maximum CO_2 saturation versus maximum CO_2 flow rate for Berea and Nugget sandstone cores.

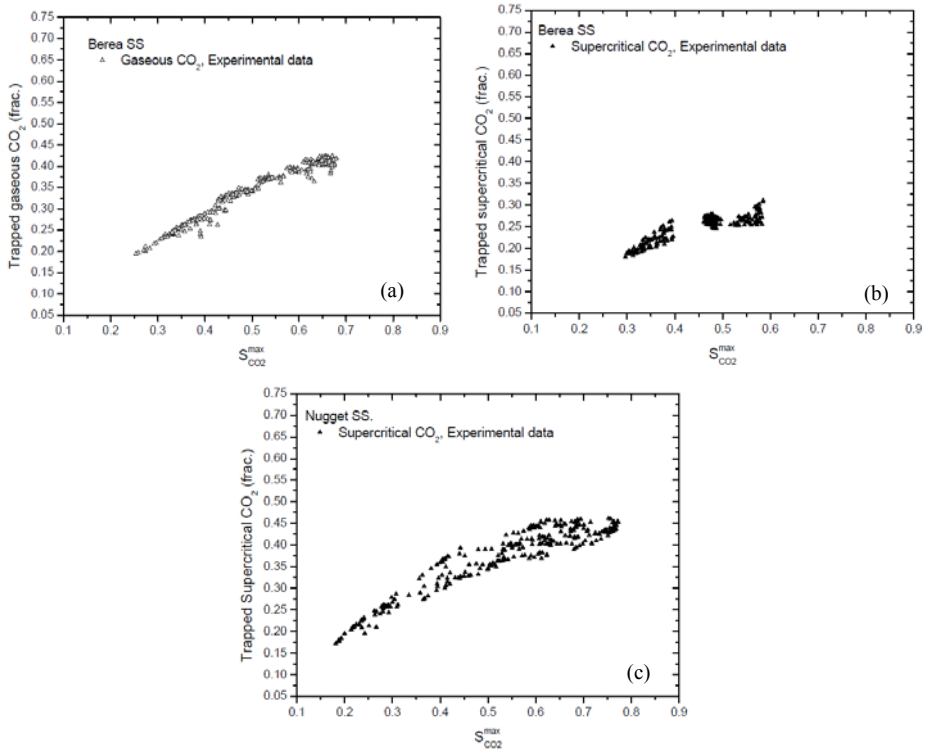

Figure 3. Variation of residual CO_2 saturation with initial CO_2 saturation in Berea and Nugget sandstone cores.

Berea Sandstone						
	84 mm from inlet		70 mm from inlet		40 mm from inlet	
Flow rate	S_{CO2}^{max}(1-S_{wirr})	S_{CO2r}	S_{CO2}^{max} (1-S_{wirr})	S_{CO2r}	S_{CO2}^{max} (1-S_{wirr})	S_{CO2r}
Q_{CO2}^{max}= 0.25 cc/min	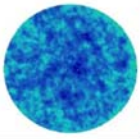	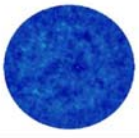	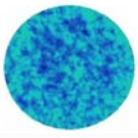		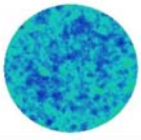	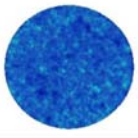
Saturation	0.331	0.1994	0.3327	0.209	0.3944	0.272
Q_{CO2}^{max} = 5.0 cc/min	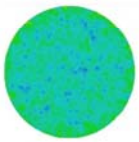	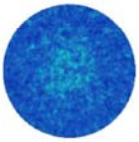	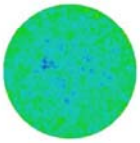	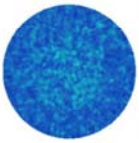	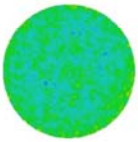	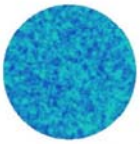
Saturation	0.4866	0.2604	0.4846	0.2776	0.5306	0.3326
Q_{CO2}^{max}= 20 cc/min	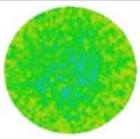	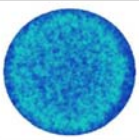	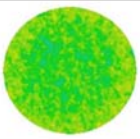	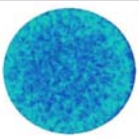	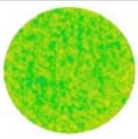	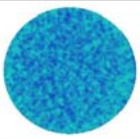
Saturation	0.6011	0.314	0.6112	0.3411	0.6568	0.356

Figure 4. CO_2 saturation distribution at different locations along the Berea core.

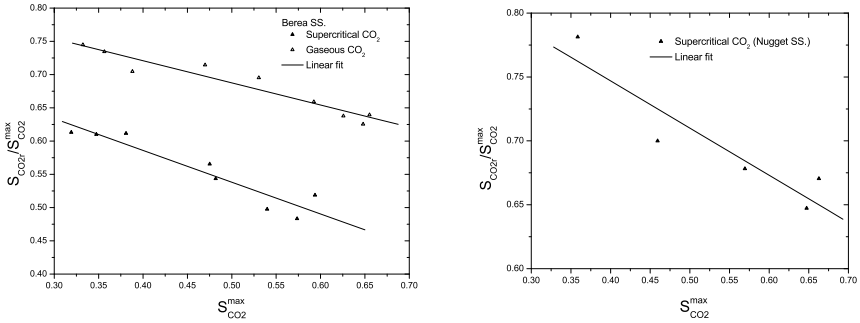

Figure 5. Trapping efficiency for Berea and Nugget sandstone.

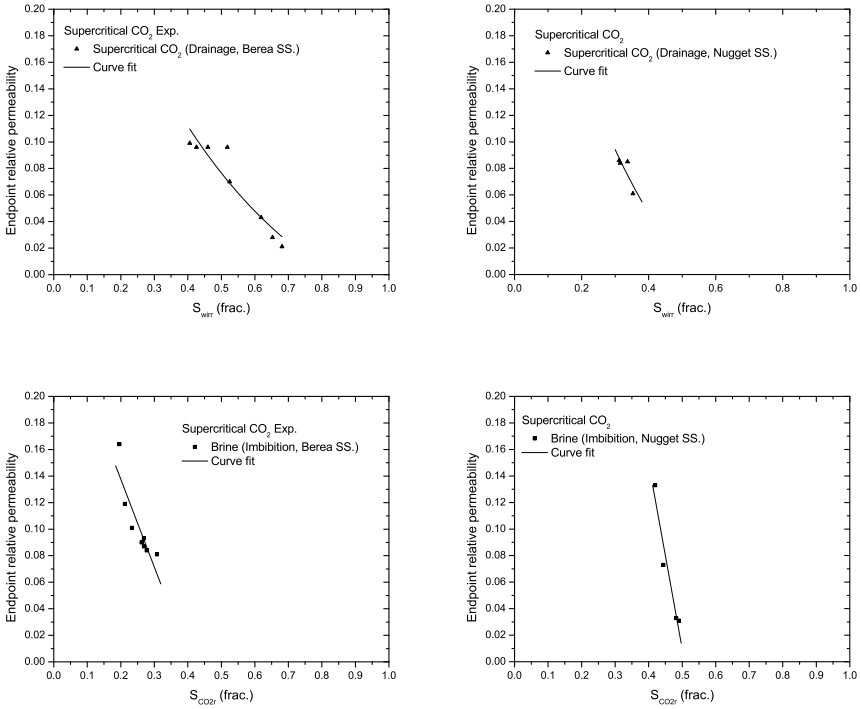

Figure 6 . Endpoints relative permeabilities for Berea and Nugget sandstone cores.

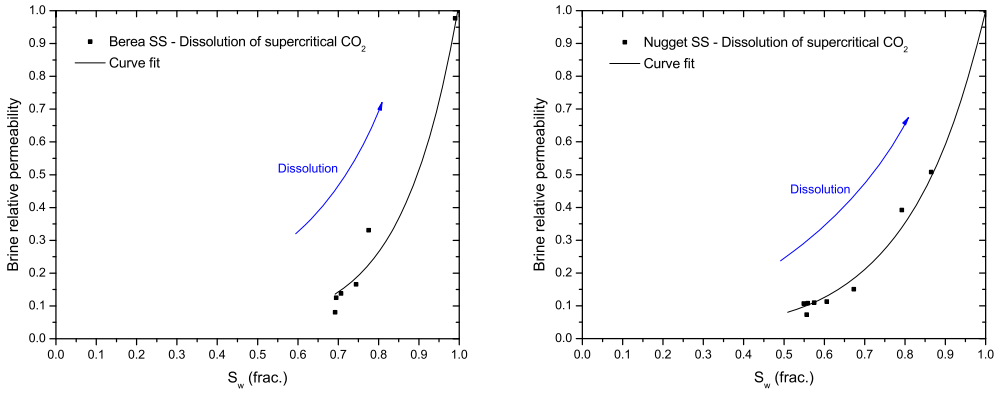

Figure 7. Brine relative permeability during dissolution process for Berea and Nugget sandstone cores**.**

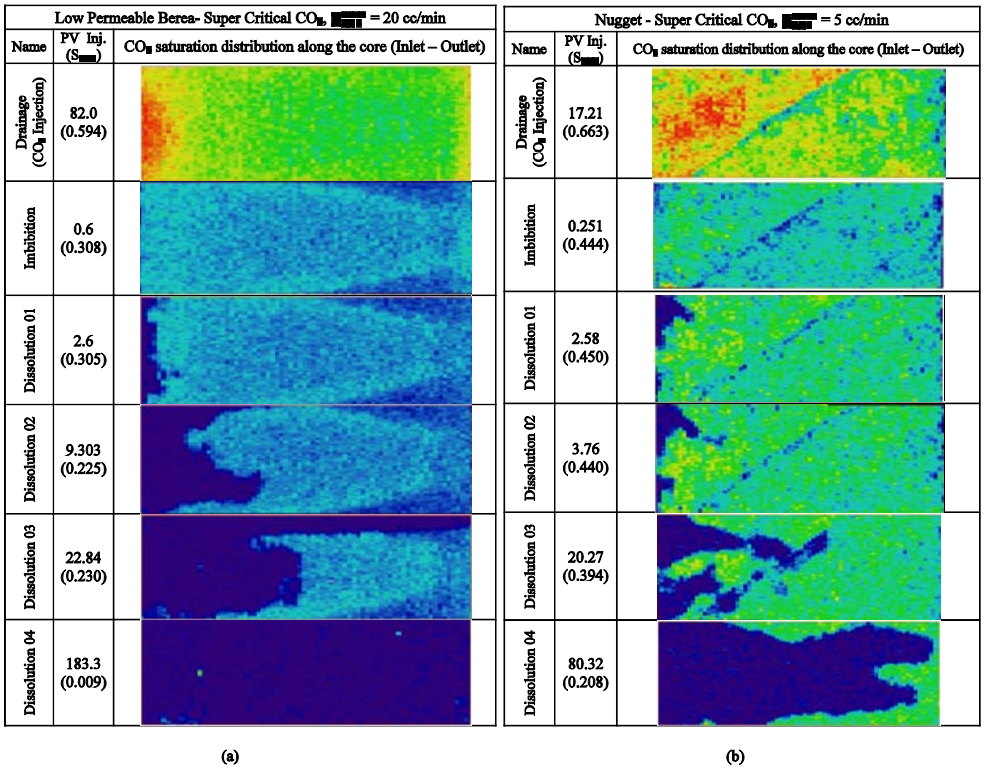

Figure 8. CO_2 saturation along the core during dissolution process in Berea and Nugget sandstone cores.